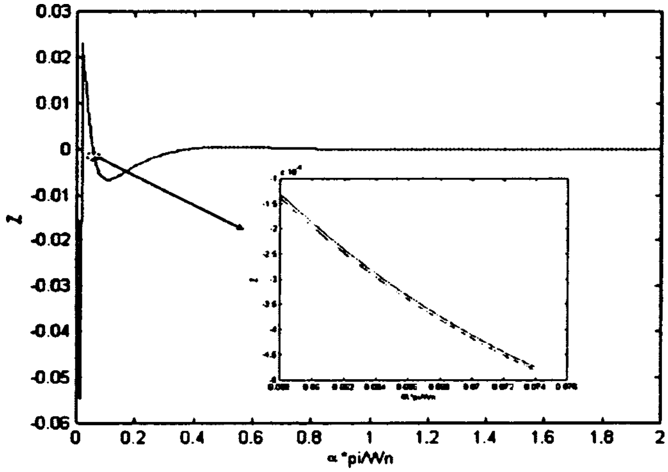

Fig. 6. Comparison of $Z_{\nu a}^{xx}$ and (10). $\nu = 10$, $p = 10$, $\epsilon_1 = 8$, $(W_m/H) = (1/2)$, and $f = 11.8$ GHz (dashed–dotted line: for (10), solid-line: our proposed method $Z_{\nu a}^{xx}$).

TABLE I
EFFECTIVE DIELECTRIC-CONSTANT COMPARISON WITH $\epsilon_1 = 8$, $2W_m/H = 1$, and $\mu_r = 1$

$\frac{H}{\lambda_o}$	This work	[3]	[10]
0.005	5.4678	5.4678	5.4752
0.05	6.1274	6.1275	6.1316
0.1	6.7582	6.7580	6.7572
0.3	7.661	7.6614	7.6551
0.7	7.9133	7.9139	7.9151
1.0	7.9529	7.9529	7.9556

for both J_x and J_y. The agreement between this paper and that presented in [3] is excellent. The total time taken to compute the effective dielectric constant for the case of $H/\lambda_o = 1$ is 4 s on a Pentium 400-MHz personal computer.

V. CONCLUSION

In this paper, the Sonie–Schafheitlin integration formula and the sampling theorem have been integrated into the conventional spectral-domain method to form an efficient and fast convergent hybrid method. Closed-form asymptotic integrals are first derived without introducing any numerical pathologies and complexities. Numerical results obtained from this approach agree very well with those reported in the literature. A substantial reduction in CPU time is also achieved using this formulation.

REFERENCES

[1] S. O. Park and C. A. Balanis, "Analytical technique to evaluate the asymptotic part of the impedance matrix of Sommerfeld-type integrals," *IEEE Trans. Antennas Propagat.*, vol. 45, pp. 798–805, May 1997.

[2] ——, "Dispersion characteristic of open microstrip lines using closed-form asymptotic extraction," *IEEE Trans. Microwave Theory Tech.*, vol. 45, pp. 458–460, Mar. 1997.

[3] S. Amari, R. Vahldieck, and J. Bornemann, "Using selective asymptotics to accelerate dispersion analysis of microstrip lines," *IEEE Trans. Microwave Theory Tech.*, vol. 46, pp. 1024–1027, July 1998.

[4] K. Uchida, T. Noda, and T. Matsunaga, "New type of spectral-domain analysis of a microstrip line," *IEEE Trans. Microwave Theory Tech.*, vol. 37, pp. 947–952, June 1989.

[5] T. Itoh, "Spectral domain immittance approach for dispersion characteristics of a generalized printed transmission lines," *IEEE Trans. Microwave Theory Tech.*, vol. MTT-28, pp. 733–736, July 1980.

[6] B. L. Ooi, P. S. Kooi, and M. S. Leong, "Efficient evaluation of singular and infinite integrals using the ERF transform," *IEEE Trans. Antennas Propagat.*, submitted for publication.

[7] G. N. Watson, *A Treatise on the Theory of Bessel Functions*. Cambridge, U.K.: Cambridge Univ. Press, 1962.

[8] I. S. Gradshteyn and I. M. Ryzhik, *Table of Integrals, Series, and Products*. New York: McGraw-Hill, 1962.

[9] M. Kobayashi and F. Ando, "Dispersion characteristics of open microstrip lines," *IEEE Trans. Microwave Theory Tech.*, vol. MTT-35, pp. 101–105, Feb 1987.

[10] S. O. Park and C. A. Balanis, "Dispersion characteristics of open microstrip lines using closed-form asymptotic extraction," *IEEE Trans. Microwaves Theory Tech.*, vol. 45, pp. 458–460, Mar 1997.

Scattering Matrices Representing the Transformations Between Modal Bases in Rectangular Waveguide

A. Morini, T. Rozzi, and L. Zappelli

***Abstract*—The excitation of hybrid modes by discontinuities in rectangular waveguide can often be decomposed into separate LSE/LSM or TE/TM mechanisms, so that each component can be analyzed with the most suitable modal base. Correct interfacing, however, is required. We report the scattering matrices representing all the possible transformations of modal bases in rectangular waveguide. Such matrices provide an useful tool to simulate complex circuits made up of components strongly interacting, without requiring the use of a common modal base for the characterization of each element. Since the transformation matrices can easily include pieces of transmission lines, their use does not require any additional computation effort.**

***Index Terms*—Mode matching, rectangular waveguides.**

I. INTRODUCTION

The electromagnetic (EM) field into a rectangular waveguide can be expanded into three different sets of modes, namely $\mathbf{H}$ and $\mathbf{E}$ types with respect to $\hat{\mathbf{x}}$, $\hat{\mathbf{y}}$, and $\hat{\mathbf{z}}$ (the latter are the classical TE/TM modes). However, although in principle any one is equivalent to another, in practical use, the analysis and computation effort required to characterize monodimensional discontinuities, such as T/Y-junctions, inductive or capacitive posts and windows, bends, tapers, and so on (see Fig. 1) is strongly reduced when the most appropriate set is used [1]. The latter is the one whose modes are derived from two potentials ($\mathbf{H}$ and $\mathbf{E}$) parallel to the axis of the discontinuity (that is, the one with respect to which the discontinuity is uniform). As a consequence, the complete analysis of the discontinuity can be performed considering separately the two families of modes ($\mathbf{E}$ and $\mathbf{H}$), as not being coupled at all by the discontinuity.

Consequently, the EM problem posed by such structures reduces to a scalar one, as the continuity condition at the discontinuity interface involves only one potential directed along one coordinate and its first derivative at a time.

On the other hand, in complex structures, there are many discontinuities and components connected together and often strongly interacting through higher order modes. A classical example of this situation is of-

Manuscript received January 13, 2000. This work was supported in part by the Agenzia Spaziale Italiana.

The authors are with the Dipartimento di Elettronica ed Automatica, Universita di Ancona, I-60131 Ancona, Italy.

Publisher Item Identifier S 0018-9480(01)00004-7.

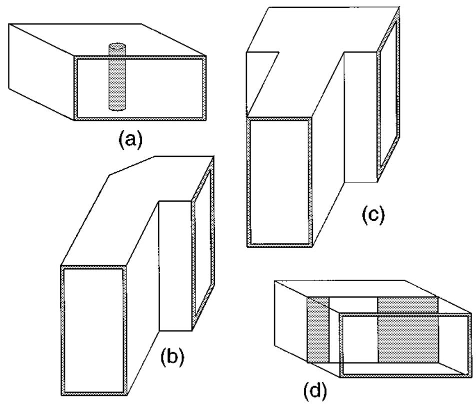

Fig. 1. Some examples of common waveguide components uniform along one direction. (a) Inductive round post. (b) $\mathbf{E}$-plane mitered bend. (c) $\mathbf{E}$-plane T-junction. (d) Inductive window.

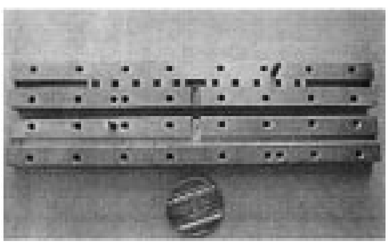

Fig. 2. Ka-diplexer consisting of an $\mathbf{E}$-plane three-port junction connected to two $\mathbf{E}$-plane septate filters. Due to the different uniformities, it is advantageous to study the two structures by means of two different modal bases.

fered by the Ka-diplexer, shown in Fig. 2. It consists of two septate filters connected to the arms of an $\mathbf{E}$-plane T-junction. Due to the uniformity of septa and junction with respect to two directions orthogonal to each other, the two modal bases suited to solve each problem are different. Of course, if the spacing between the first septum of filters and the junction is large enough (at least one waveguide width a), interaction occurs only via the fundamental mode, and the connection of the two models, although based on different modes, does not pose any problem. Often, however, such distance is shorter than a and higher order modes interaction has to be taken into account. A possible solution to this problem, the most commonly used indeed, consists of employing the same modal base, typically TE and TM modes ($\mathbf{H}$ and $\mathbf{E}$ modes with respect to $\hat{\mathbf{z}}$) for both cases, as the resulting scattering matrices can be connected directly. The drawback of such an approach is that it does not take advantage of the uniformity of each discontinuities and the resulting EM problem, i.e., the continuity of the tangential EM field at the discontinuity interfaces, involves vector, instead of scalar, fields.

This, of course, implies losing compactness in formulation and efficiency in the numerical solution. In addition, sometimes one has to connect scattering matrices resulting from different EM simulators, not always sharing the same modal bases.

It is also apparent that a major limitation of some otherwise excellent computer-aided design (CAD) tools and EM simulators is often caused by the impossibility of connecting $\mathbf{E}$- and $\mathbf{H}$-plane circuits with pieces of waveguide unless the interconnecting waveguides are long enough (at least one waveguide width), as those codes are unable to manage the interactions between different families of modes [2].

This paper provides a solution to this problem by showing how to connect scattering matrices deriving from different modal bases by means of the matrices representing the transformation of one modal base into another one.

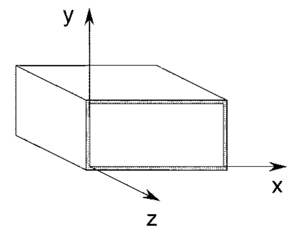

Fig. 3. Section of a rectangular waveguide showing the coordinate system.

Such matrices have the form of a generalized scattering matrix and can be handled as any junction. It is, therefore, possible to analyze a complex structure, consisting of the interconnection of many junctions, while characterizing each junction with its more appropriate modal base [1] and connecting the elementary junctions by the interposition of such transformation matrices when the adjacent junctions are analyzed with distinct modal bases.

We will call such matrices *transformation scattering matrices* or, more briefly, τ matrices.

Moreover, since the junctions are always separated by pieces of waveguides, the τ matrices can be easily modified to include pieces of lines in such a way that just one τ matrix represents both the change of modal base and the connecting lines. Thus, the use of a τ matrix has the same computational cost as that of a (generalized) transmission line.

II. Derivation of the τ Matrices

A complete modal base to represent the field into a rectangular waveguide can be derived from two Hertzian potentials Π_e and Π_h, both directed as either $\hat{\mathbf{x}}$ or $\hat{\mathbf{y}}$ or $\hat{\mathbf{z}}$ (Fig. 3)

$$\Pi_e = \psi_e(x,\, y)e^{\mp\gamma z}\hat{\mathbf{u}} \tag{1}$$
$$\Pi_h = \psi_h(x,\, y)e^{\mp\gamma z}\hat{\mathbf{u}} \tag{2}$$

where $\hat{\mathbf{u}}$ is either $\hat{\mathbf{x}}$ or $\hat{\mathbf{y}}$ or $\hat{\mathbf{z}}$, $\gamma^2 = k_{tnm}^2 - k_0^2$, $k_{tnm}^2 = (n\pi/a)^2 + (m\pi/b)^2$, a, b are the dimensions of the transverse waveguide section, and k_0 is the wavenumber in the free space. The upper sign refers to positive traveling waves, the lower to the negative ones.

In order to correctly represent a given modal base into another, it is essential to choose the sign of the Hertzian potentials in such a way that the resulting transverse modal fields take the following form:

$$\mathbf{E}_{t\lambda}(x,\, y,\, z) = a_1\mathbf{e}_\lambda(x,\, y)e^{-\gamma z} + b_1\mathbf{e}_\lambda(x,\, y)e^{+\gamma z} \tag{3}$$
$$\mathbf{H}_{t\lambda}(x,\, y,\, z) = a_1\mathbf{h}_\lambda(x,\, y)e^{-\gamma z} - b_1\mathbf{h}_\lambda(x,\, y)e^{+\gamma z} \tag{4}$$

where $\mathbf{e}_\lambda(x,\, y)$, $\mathbf{h}_\lambda(x,\, y)$ are the transverse electric and magnetic modal functions, normalized in such a way that

$$\int_{\text{cross section}} \mathbf{e}_\lambda \times \mathbf{h}_\mu \cdot\, d\mathbf{s} = \delta_{\lambda\mu} \tag{5}$$

λ and μ are global indexes, standing for the polarization ($\mathbf{E}/\mathbf{H}$) and the eigenvalue k_{tnm}.

This means that the potential are normalized in such a way that a modal wave propagating in the positive direction differs from one propagating in the negative direction just for the sign of the transverse magnetic field. *Note also that the normalization condition (5) only holds for modal functions deriving from vector potentials that are parallel.*

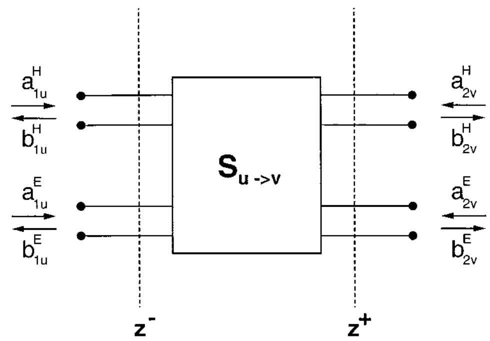

Fig. 4. τ matrix represents the transformation of one modal base into another at an arbitrary waveguide section z.

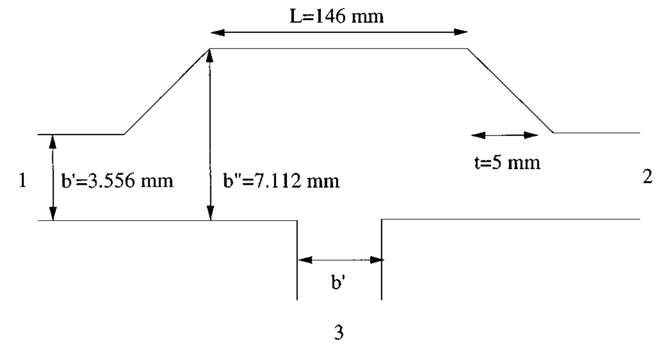

Fig. 5. **E**-plane section of an oversize T-junction terminated on standard waveguides via two tapers. The sketch is not on scale.

According to the above assumption, the scalar functions ψ's appearing in (1) and (2) assume the following forms.

$\mathbf{E}$, $\mathbf{H}$ modes with respect to $\hat{\mathbf{x}}$ ($\mathrm{LSM}_x, \mathrm{LSE}_x$)

$$\psi_e(x,\, y) = \pm\, A_{ex} \cos k_x x \sin k_y y \tag{6}$$

$$\psi_h(x,\, y) = A_{hx} \sin k_x x \cos k_y y. \tag{7}$$

$\mathbf{E}$, $\mathbf{H}$ modes with respect to $\hat{\mathbf{y}}$ ($\mathrm{LSM}_y, \mathrm{LSE}_y$)

$$\psi_e(x,\, y) = \mp\, A_{ey} \sin k_x x \cos k_y y \tag{8}$$

$$\psi_h(x,\, y) = A_{hy} \cos k_x a x \sin k_y y. \tag{9}$$

$\mathbf{E}$, $\mathbf{H}$ modes with respect to $\hat{\mathbf{z}}$ (TM, TE)

$$\psi_e(x,\, y) = A_{ez} \sin k_x x \sin k_y y \tag{10}$$

$$\psi_h(x,\, y) = \mp\, A_{hz} \cos k_x x \cos k_y y. \tag{11}$$

The expressions of the normalization constants A's are reported in the Appendix. As usual, $k_x = (n\pi/a)$, $k_y = (m\pi/b)$.

Once the normalized modal vectors $\mathbf{e}_u^{p_u}$, $\mathbf{h}_u^{p_u}$, p_u indicating the polarization, either $\mathbf{H}$ or $\mathbf{E}$, of the potential directed along $\hat{\mathbf{u}}$, have been calculated in the classical way for each Hertzian potential [3], it is immediate to compute the coupling coefficients $s_{uv}^{p_u,\,p_v}$ between two modes, both corresponding to the same eigenvalue k_{tnm}, deriving from potentials directed along $\hat{\mathbf{u}}$ and $\hat{\mathbf{v}}$, respectively,

$$s_{uv}^{p_u,\,p_v} = \int_{\text{cross section}} \mathbf{e}_u^{p_u} \times \mathbf{h}_v^{p_v} \cdot d\mathbf{s}. \tag{12}$$

The calculation of the coupling coefficients is straightforward and produces as a result the τ-scattering matrices $\mathbf{S}_{\mathbf{u}\to\mathbf{v}}$ representing the transformation of the modes derived from two potentials directed along one direction, say, $\hat{\mathbf{u}}$, to the ones derived from another direction $\hat{\mathbf{v}}$.

In other words, the above matrix represents a junction actually located at a given waveguide section z. The waves incident into ports 1 (modes $\mathbf{H}$ and $\mathbf{E}$ with respect to $\hat{\mathbf{u}}$) and 2 (modes $\mathbf{H}$ and $\mathbf{E}$ with respect to $\hat{\mathbf{v}}$), are linked to the ones reflected at the same ports, as shown in Fig. 4. Considering the (4 × 4) block corresponding to the eigenvalue k_{tnm}, we have

$$\begin{bmatrix} b_{1u}^H \\ b_{1u}^E \\ b_{2v}^H \\ b_{2v}^E \end{bmatrix} = \mathbf{S}_{\mathbf{u}\to\mathbf{v}} \begin{bmatrix} a_{1u}^H \\ a_{1u}^E \\ a_{2v}^H \\ a_{2v}^E \end{bmatrix} \tag{13}$$

where

$$\mathbf{S}_{\mathbf{u}\to\mathbf{v}} = \begin{bmatrix} \mathbf{0} & \mathbf{S}_{uv} \\ \mathbf{S}_{uv}^T & \mathbf{0} \end{bmatrix}. \tag{14}$$

It is easy to recognize that the forward and reverse transformation matrices are linked to each other by the following:

$$\mathbf{S}_{\mathbf{v}\to\mathbf{u}} = \mathbf{S}_{\mathbf{u}\to\mathbf{v}}^T. \tag{15}$$

Thus, the expressions of the τ matrices are as follows:

$$\mathbf{S}_{zx} = \frac{1}{\sqrt{(k_0^2 - k_x^2)(k_x^2 + k_y^2)}} \begin{bmatrix} j\gamma k_x & -k_0 k_y \\ -k_0 k_y & -j\gamma k_x \end{bmatrix} \tag{16}$$

$$\mathbf{S}_{zy} = \frac{1}{\sqrt{(k_0^2 - k_y^2)(k_x^2 + k_y^2)}} \begin{bmatrix} j\gamma k_y & k_0 k_x \\ k_0 k_x & -j\gamma k_y \end{bmatrix} \tag{17}$$

$$\mathbf{S}_{xy} = \frac{1}{\sqrt{(k_0^2 - k_y^2)(k_0^2 - k_x^2)}} \begin{bmatrix} -k_x k_y & j\gamma k_0 \\ -j\gamma k_0 & -k_x k_y \end{bmatrix}. \tag{18}$$

As can be observed, the above matrices represent an ideal transition between two different families of modes. It is evident that $\mathbf{S}_{uu}$ is the unit matrix $\mathbf{U}$, and it can also be easily verified that

$$\mathbf{S}_{\mathbf{u}\to\mathbf{v}} \odot \mathbf{S}_{\mathbf{v}\to\mathbf{u}} = \begin{bmatrix} \mathbf{0} & \mathbf{U} \\ \mathbf{U} & \mathbf{0} \end{bmatrix} \tag{19}$$

where the symbol $\odot$ indicates the operation of cascade connection of two networks represented by their scattering matrices.

Of course, the following property also holds:

$$\mathbf{S}_{\mathbf{u}\to\mathbf{v}} \odot \mathbf{S}_{\mathbf{v}\to\mathbf{w}} = \mathbf{S}_{\mathbf{u}\to\mathbf{w}}. \tag{20}$$

Commonly, in microwave circuits, one has to connect two discontinuities or circuits separated by a length l of waveguide.

In this case, the transformation matrix ought to be able to include the length of waveguide too. This is easy to obtain, simply by multiplying each block (one for each eigenvalue) of the transformation matrix for the propagation term

$$\mathbf{S}_{uv}^l = \mathbf{S}_{uv} e^{-\gamma l}. \tag{21}$$

Therefore, the τ matrix can be seen as a generalization of the generalized scattering matrix (GSM) representing a piece of waveguide that, in addition, provides a modal transformation.

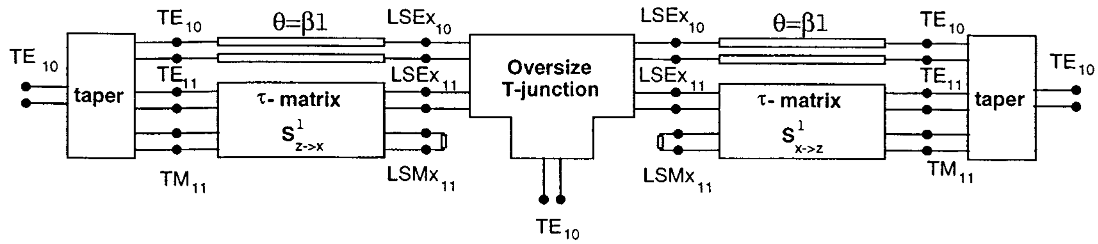

Fig. 6. Equivalent network model of the oversized T-junction. The τ matrix permits the connection between modes having the same indexes, but deriving from different potentials. As known, TE_{10} and LSE_{10} modes are equivalent and their connection does not require the interposition of a τ matrix.

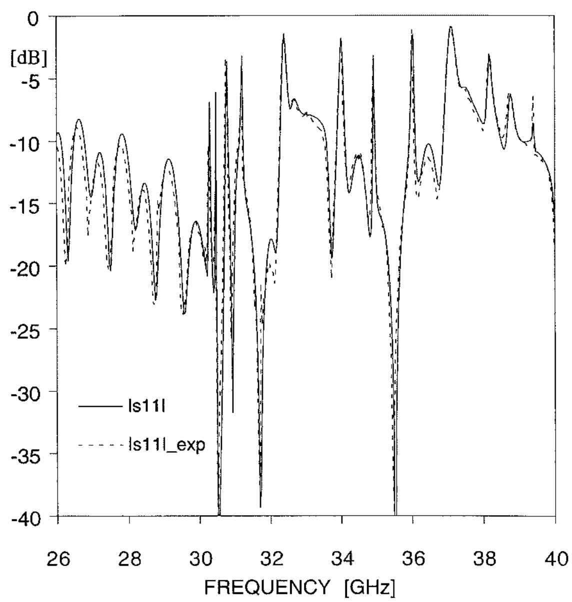

Fig. 7. Comparison between the theoretical and experimental reflections at port 1 of the oversized T-junction shown in Fig. 5.

III. Example

As an example of application of the above theory, we consider a component given by the connection between a WR28 $\mathbf{E}$-plane oversized T-junction and two tapered sections, as sketched in Fig. 5. Three modes, i.e., TE_{10}, TE_{11}, and TM_{11}, can propagate through the oversize section $(b'' = 2b')$ over the waveguide band. On the other hand, being both the three-port junction and the tapers uniform with respect to x, they could be conveniently analyzed considering separately the LSE_x and LSM_x cases. In both cases, the EM problem is scalar as involving the continuity at the discontinuity interfaces of E_y and H_x in the LSE_x case, and the continuity of H_y and E_x, in the LSM_x case. In addition, the analysis under LSE_x excitation suffices for a complete characterization of the junction because, due to the uniformity with respect to x, LSM_x modes are not excited at all. In our case, the GSM of the tapers derives from HFSS[1] and it is expressed in terms of TE and TM modes. The GSM of the three-port junction, modeled by ourselves, is expressed in terms of the most appropriate modal base, i.e., the LSE_x. In order to connect the two GSMs, we have to insert them between the τ-matrix introduced in this paper representing the transformation TE/TM into $\mathrm{LSE}_x/\mathrm{LSM}_x$. Moreover, the two pieces of oversized waveguide of length l, separating the three-port junction and the tapers, are automatically taken into account considering the τ-matrix in the form of (21).

The physical situation is represented by the circuit shown in Fig. 6. Finally, note that the LSM_{11} mode is terminated by a matched load, as it is not actually excited by the structure. For the sake of brevity, only the reflection at one port is shown in Fig. 7. The agreement between theoretical and experimental data is due both to the accuracy of the EM analysis of each individual block and to the correctness of the proposed τ-matrix.

IV. Conclusions

Transformation matrices permit to connect GSMs representing waveguide components, when they are modeled starting from different modal bases. Their use is particularly effective, as they can be considered a generalization of a GSM representing a length of waveguide, with the additional feature that the modal base at the input is different from that at the output.

Appendix

The expressions of the modal normalization constants are as follows:

$$A_{ex} = \frac{\epsilon_n \epsilon_m}{\sqrt{ab}} \left[-j\omega\epsilon\gamma\left(k_0^2 - k_x^2\right)\right]^{-1/2} \tag{22}$$

$$A_{hx} = \frac{\epsilon_n \epsilon_m}{\sqrt{ab}} \left[-j\omega\mu_0\gamma\left(k_0^2 - k_x^2\right)\right]^{-1/2} \tag{23}$$

$$A_{ey} = \frac{\epsilon_n \epsilon_m}{\sqrt{ab}} \left[-j\omega\epsilon\gamma\left(k_0^2 - k_y^2\right)\right]^{-1/2} \tag{24}$$

$$A_{hy} = \frac{\epsilon_n \epsilon_m}{\sqrt{ab}} \left[-j\omega\mu_0\gamma\left(k_0^2 - k_y^2\right)\right]^{-1/2} \tag{25}$$

$$A_{ez} = \frac{\epsilon_n \epsilon_m}{\sqrt{ab}} \left[j\omega\epsilon\gamma\left(k_x^2 + k_y^2\right)\right]^{-1/2} \tag{26}$$

$$A_{hz} = \frac{\epsilon_n \epsilon_m}{\sqrt{ab}} \left[j\omega\mu_0\gamma\left(k_x^2 + k_y^2\right)\right]^{-1/2} \tag{27}$$

where $\epsilon_0 = 2$ and $\epsilon_k = \sqrt{2}$ for $k \neq 0$.

References

[1] H. M. Altshuler and L. O. Goldstone, "On network representation of certain obstacles in waveguide regions," *IRE Trans. Microwave Theory Tech.*, vol. 7, no. MTT-4, pp. 213–221, Apr. 1959.

[2] P. Arcioni, M. Bressan, G. Conciauro, L. Perregrini, and G. Gatti, "ANAPLAN-W: A CAD tool for E/H-plane waveguide circuits," *ESA J.*, vol. 6, no. 1, pp. 12–13, Mar. 1996.

[3] R. Collin, *Field Theory of Guided Waves*, II ed. Piscataway, NJ: IEEE Press, 1993.

[1]HFSS Beta version 6.0.02, Ansoft Corporation ©1994–1998.